

Fire Detection Based on Improved HOG

Min Yan^{1,2}

¹College of Computer Science&Technology
Nanjing Tech University
Nanjing, China

²Faculty of Computer & Software Engineering
Huaiyin Institute of Technology
Huaian, China
email: yanminfpt@126.com

Yunyang Yan^{1,2}

¹College of Computer Science&Technology
Nanjing Tech University
Nanjing, China

²Faculty of Computer & Software Engineering
Huaiyin Institute of Technology
Huaian, China
email: yunyang@hyit.edu.cn

Abstract—Rules in color model is an important method to identify candidate fire region. If the candidate fire region is not correct, the features extracted in subsequent steps are wrong. In this paper, a combination of constraint rules based on RGB and YCbCr color model is proposed. Compared with the constraint rules based on the YCbCr color model of other references, the proposed method extracts less noise from the candidate fire region, whether it is a fire picture or a non-fire picture. The HOG feature can not only detect the edge part of the object well, but also quantify the distribution structure of pixels inside the object through the distribution of statistical gradient vector angles. Based on these two advantages, this paper uses the HOG feature for fire detection. Scanning the entire image with overlap, the HOG feature vector dimension of the image is too large. Time complexity of fire detection is higher. This paper improves it and combines multiple features to detect fire. The average detection rate for fire video is 96.1%, and the average detection rate for none-fire video reached 100%.

Keywords- Fire; YCbCr; HOG; Multiple Features

I. INTRODUCTION

With the development of machine learning, video-based fire detection becomes more and more popular. Reference [1] proposed constraint rules in RGB to extract suspected fire region. Reference [2] input the image, determines whether the image satisfies the constraint rules in the RGB space and satisfies the constraint rule of the YCbCr space, and if both are satisfied, the pixel is determined to be a fire candidate region. Reference [3] uses the constraint rules in the YCbCr and HSV color spaces to segment fire area. Reference [4] uses constraint rules to extract candidate regions in HSI space, and combines optical flow method to divide motion vectors into 8 directions to detect fire. The fire detection model in reference [5] uses spatiotemporal visual saliency to detect fire, extracting candidate regions in Lab space and using thresholds and Gaussian filters to segment the fire candidate regions.

After segmenting the candidate fire region, features are fed into the classifier for training and recognition.

Area, centroid coordinates, mean and standard deviation of Cb and Cr components in YCbCr are extracted to form a 7-dimensional feature vector [6]. In reference [7], circularity, rectangularity, center of gravity height coefficient, the ratio of length to width, shape of boundary roughness

characteristics and LBP (Local Binary Patterns) are extracted into GBDT (Gradient Boosting Decision Tree) to recognize fire. In reference [8], flicker, fraction dimension, LBP, etc. are used to detect fire image. In reference [9], circularity, rectangularity, center-of-gravity height coefficients and LBP are fused into feature vector to be trained and to detect fire.

II. RULES IN COLOR MODEL

A. Rules in YCbCr and RGB Color Model

YCbCr color model can isolate luminance from chrominance contrasted with RGB color model. 'Y' represents luminance, 'Cb' represents chrominance blue and 'Cr' represents red minus luminance. The formula for conversion from RGB to YCbCr is shown in Eq. (1).

$$\begin{pmatrix} Y \\ Cb \\ Cr \end{pmatrix} = \begin{pmatrix} 0.2568 & 0.5041 & 0.0979 \\ -0.1482 & -0.2910 & 0.4392 \\ 0.4392 & -0.3678 & -0.0714 \end{pmatrix} \begin{pmatrix} R \\ G \\ B \end{pmatrix} + \begin{pmatrix} 16 \\ 128 \\ 128 \end{pmatrix} \quad (1)$$

Reference [2] proposes constraint rules on RGB and YCbCr spaces, and the formula is given in Eq.(2).

$$\begin{cases} rule1 : Y(x, y) \geq Cb(x, y) \geq Cr(x, y) \\ rule2 : R(x, y) > G(x, y) > B(x, y) \\ rule3 : R(x, y) \geq RTH \end{cases} \quad (2)$$

The constraint rules based on YCbCr color model is shown in Eq.(3)[10].

$$\begin{cases} rule1 : |Cb(x, y) - Cr(x, y)| > T \\ rule2 : Y(x, y) > Cb(x, y) \\ rule3 : Cr(x, y) > Cb(x, y) \end{cases} \quad (3)$$

B. Proposed Rules in RGB and YCbCr Color Model

Reference [2] and Reference [10] have the problem of inaccurate extraction of candidate fire regions by experiments. Aiming at this problem, the YCbCr space is first improved and combined with RGB space. Constraint rules are proposed. Improved YCbCr color space is shown in Eq.(4).

$$\begin{pmatrix} Y^\# \\ Cb^\# \\ Cr^\# \end{pmatrix} = \begin{pmatrix} 0.2568 & 0.5041 & 0.0979 \\ -0.1482 & -0.2910 & 0.4392 \\ 0.4392 & -0.3678 & -0.0714 \end{pmatrix} \begin{pmatrix} R \\ G \\ B \end{pmatrix} \quad (4)$$

Constraint rules based on RGB and YCbCr space is shown in Eq.(5).

$$\begin{cases} \text{rule1} : Y^\#(x, y) > Y^\#_{mean} \\ \text{rule2} : Cb^\#(x, y) < Cb^\#_{mean} \\ \text{rule3} : Cr^\#(x, y) > Cr^\#_{mean} \\ \text{rule4} : Y^\#(x, y) > Cb^\#(x, y) \\ \text{rule5} : R(x, y) > RTH \end{cases} \quad (5)$$

In formula (6), RTH is the threshold of the R channel. M and N are the length and width of the image.

$$\begin{cases} Y^\#_{mean} = \frac{\sum_{x=1}^M \sum_{y=1}^N Y^\#(x, y)}{M \times N} \\ Cb^\#_{mean} = \frac{\sum_{x=1}^M \sum_{y=1}^N Cb^\#(x, y)}{M \times N} \\ Cr^\#_{mean} = \frac{\sum_{x=1}^M \sum_{y=1}^N Cr^\#(x, y)}{M \times N} \\ RTH = 140 \end{cases} \quad (6)$$

The binary images from different constraint rules are shown in Figure 1.

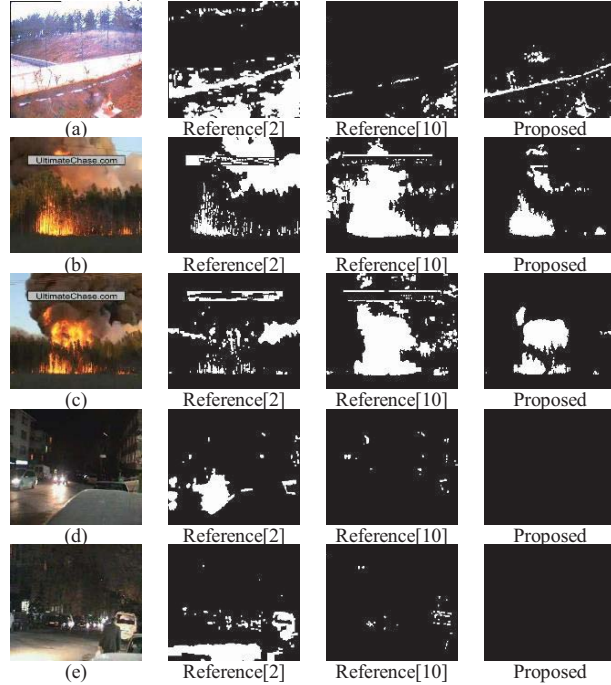


Figure 1. Binary Images Obtained by Different Rules

The fire candidate region extracted by this proposed method is more accurate, especially for none-fire images in Figure 1.

III. HOG FEATURE

A. HOG

HOG(Histograms of Oriented Gradients) was proposed to initially detect humans [11]. Firstly, calculate the value of the pixel point in the image $f(x, y)$ in the x direction, the formula is shown in Eq.(7).

$$G_x(x, y) = f(x + 1, y) - f(x - 1, y) \quad (7)$$

Secondly, calculate the change of pixel point of image $f(x, y)$ in y direction, the formula is shown in Eq.(8).

$$G_y(x, y) = f(x, y + 1) - f(x, y - 1) \quad (8)$$

The gradient vector angle of pixel is shown in Eq.(9).

$$a(x, y) = \tan^{-1} \left(\frac{G_y(x, y)}{G_x(x, y)} \right) \quad (9)$$

The gradient vector modulus of pixel is shown in Eq.(10).

$$G(x, y) = \sqrt{G_x(x, y)^2 + G_y(x, y)^2} \quad (10)$$

B. Improved HOG

The HOG feature of reference [11] and the HOGHOF feature of reference [12] all require that the vector dimension of the repeated scan of the entire image be too large, and the feature vector dimension of HOGHOF is larger, which results in too slow processing speed and is not conducive to real-time detection of fire [12]. To solve this problem, this paper proposes improved HOG. Improved HOG uses the connected domain as a unit to distribute the weights of gradient vector angle intervals according to the gradient vector modulus of the pixels. The gradient vector angle matrix is calculated and used as the input matrix of the next layer. Each layer needs to calculate the input matrix's gradient vector angle matrix and gradient vector modulus size matrix. The flow chart is shown in Figure 1.

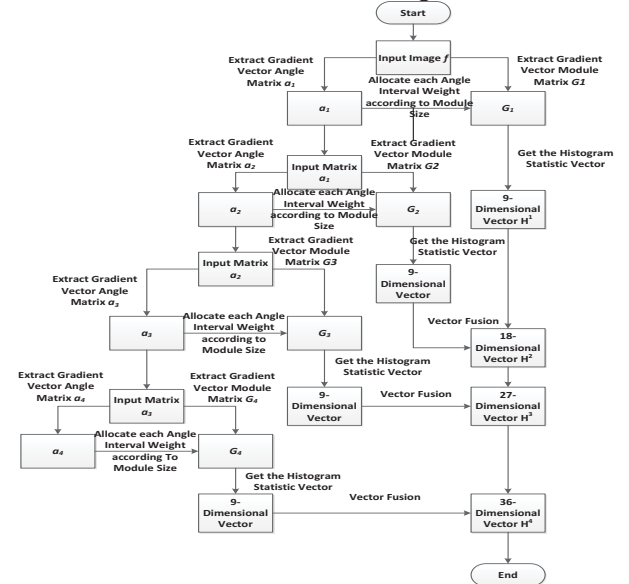


Figure 2. Improved HOG Feature Extraction Flow Chart

This paper uses 100 fire images and 100 none-fire images for train by SVM, using 300 fire images and 200 none-fire images for testing, which is shown in TABLE 1.

TABLE 1. Improved HOG Recognition Rate in Different Dimensions

Feature Combination	Number Of fire Pictures	Rate Of Fire Pictures	Number Of None-Fire Pictures	Rate Of None-Fire Pictures	Total Rate
H ¹	243	81.0	168	84.0	82.2
H ²	246	82.0	172	86.0	83.6
H ³	274	91.0	177	88.5	90.2
H ⁴	267	89.0	169	84.5	87.2

From the Table 1, we can see that with the increase of dimension of the feature vector, the recognition rate is also improved. When the vector dimension is 27, the recognition rate is the highest. This paper uses a 27-dimensional vector as the final texture extraction method.

Reference [9] uses LBP combined with multiple features for fire image detection, and the proposed method comparing with it. The recognition rate of LBP and H³ HOG is shown in TABLE 2.

TABLE 2. Recognition Rate of LBP and HOG

	Reference [9]	Proposed H ³
Recognition Rate/%	83.5	90.2
Vector Dimension	24	27

In Table 2, the H³ HOG recognition rate is higher than LBP.

Since HOGHOF's dimension is higher than the HOG vector, it's time complexity is higher. Improved HOG is compared with HOG by processing speed. The test video sequence is shown in Figure 3.



Figure 3. Test Video Sequence

The average processing time per frame for the HOG and improved H³ HOG are shown in Figure 4.

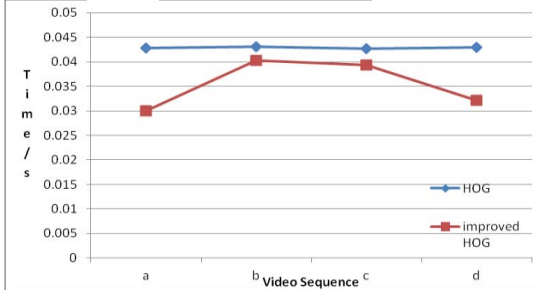


Figure 4. Time Complexity of HOG and Improved HOG

C. Multiple Features based on Improved HOG

In order to improve the recognition rate, the shape structure features of the fire can be fused together with the improved HOG features into multiple features for fire detection.

Circularity indicates whether the connected domain is similar to a circle, and L and S respectively represent the

perimeter and area. The formula of circularity is shown in Eq.(11)[9].

$$C = \frac{L^2}{4\pi \times S} \quad (11)$$

S represents the area of the connected area and S_R represents the area of the circumscribed rectangle of the connected area, the formula of rectangularity is shown in Eq.(12)[9].

$$R = \frac{S}{S_R} \quad (12)$$

L_{CH} refers to the perimeter of the convex hull of the connected domain, and L is the perimeter of the connected domain, boundary roughness is shown in Eq.(13)[9].

$$B = \frac{L}{L_{CH}} \quad (13)$$

The recognition rates of different features combinations is shown in TABLE 3.

TABLE 3. Recognition Rate of Different Feature Combinations

Feature Combination	Number of Fire Pictures	Rate of Fire Pictures	Number of None-Fire pictures	Rate of None-Fire pictures	Total Rate
C	231	77.0	105	52.5	67.2
R	253	84.0	128	64.0	76.2
B	222	74.0	127	63.5	69.8
C+R+B	251	83.7	151	75.5	80.4
C+R+B+H ¹	285	95.0	169	84.5	90.8
C+R+B+H ²	280	93.3	175	87.5	91.0
C+R+B+H ³	281	93.7	173	86.5	90.8

Considering that the color candidate region determines the shape characteristics of the fire, HOG features are relatively less affected. The combination of H³ performs well in the detection of fire and none-fire images in Table 3, H³ HOG with multiple features is used for fire video detection.

IV. EXPERIMENT AND ANALYSIS

The video comes from the Bilkent fire video library. After extracting the color region and extracting the motion region, extract the multiple features from the region and the multiple features are sent into the support vector machine for classification and discrimination. The result of experiment is shown in Figure 5.

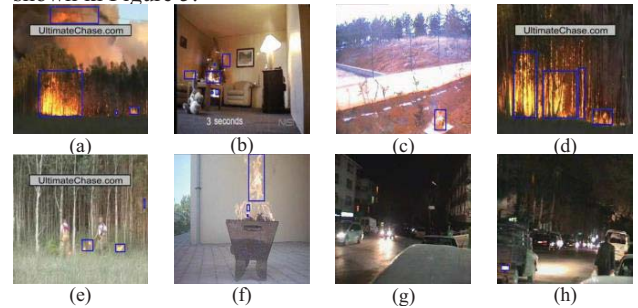


Figure 5. Result of Experiment

The fire video recognition rate is shown in TABLE 4.

TABLE 4. Fire Video Detection Results

Video	Total Frames	Reference[7]		Reference[8]		Proposed	
		TP/%	FP/%	TP/%	FP/%	TP/%	FP/%
a	190	99.1	0.9	96.5	3.5	100	0
b	75	93.6	6.4	96.0	4.0	90.1	9.9
c	400	90.9	9.1	98.0	2.0	98.4	1.6
d	208	98.8	1.2	98.0	2.0	99.3	0.7
e	260	97.6	2.4	96.5	3.5	98.1	1.9
f	707	95.6	4.4	96.0	4.0	90.9	9.1

The recognition rate of none-fire video is shown in TABLE 5.

TABLE 5. None-Fire Video Detection Results

Video	Total Frames	Reference[7]		Reference[8]		Proposed	
		TN/%	FN/%	TN/%	FN/%	TN/%	FN/%
g	144	99.3	0.7	100	0	100	0
h	149	97.3	2.7	100	0	100	0

From experiments, reference [7] uses GBDT to extract features such as circularity, rectangularity, center-of-gravity height coefficient, aspect ratio, boundary roughness, and local texture. Using random forests to perform feature combinations to find the combination with the highest recognition rate as a criterion. The features are used to identify the fire video. The recognition of video c and f is poor, because the fire of d video changes drastically and the background color is close to the fire color, resulting in the final extracted features such as circularity, rectangle, aspect ratio, etc., which are none-fire video. The recognition is more accurate because the light sources in these videos change slowly and their circularity is large, and the features are more obvious.

Reference [8] uses gradient motion to extract motion regions. First, it compares whether the pixel points of the motion region match the fire color that has been improved by k-means clustering. Secondly, compares whether the flash frequency characteristics of the region matches the fire, and then extracts the LBP feature to send it. In the SVM, the contour near each suspected pixel is analyzed based on the fractal dimension, and finally it is determined whether all the conditions are met to identify the fire. This method has the best recognition effect in none-fire video, all at 100%. This is due to the fact that the fire profile has self-similar structural features and the lamp does not contain such a structure. Therefore, on none-fire video the recognition rate is most accurate. The recognition rate for fire video c and d is higher because the fire presented by these two videos is the most complex and its fractal dimension is the most obvious.

This paper uses the morphological characteristics of fire and its own texture feature to recognize it. Using the improved HOG feature to describe the texture mathematically, the recognition effect of none-fire video is better, because the non luminous video has a smooth texture. The distribution of HOG feature gradient vectors is also more concentrated, and the recognition effect on fire video b and f is poor. This is because the fire of these two videos

change drastically and the fire color is whiter. This article does not extract dynamic features and the colors proposed in this paper. Constraint rules are not very sensitive to whiter colors.

V. CONCLUSIONS

Although the fire region extracted by the color constraint rule of this paper is more accurate and has strong anti-interference ability, the extracted fire region will be incomplete if the center portion is white. This paper proposes improved H³ HOG with multiple features. Although the recognition rate is improved, the dynamic characteristics of the fire are not effectively used. The next step is to combine the H³ HOG with dynamic features for fire detection.

REFERENCES

- [1] T.H. Chen, P.H. Wu and Y.C. Chiou, "An early fire-detection method based on image processing," Image Processing, 2004. ICIP '04. 2004 International Conference on, 2004, pp. 1707-1710 Vol. 3.
- [2] N. S. Bakri, R. Adnan, A. M. Samad and F. A. Ruslan, "A methodology for fire detection using colour pixel classification," 2018 IEEE 14th International Colloquium on Signal Processing & Its Applications (CSPA), Malaysia, 2018, pp. 94-98.
- [3] S. G. Benjamin, B. Radhakrishnan, T. G. Nidhin and L. P. Suresh, "Extraction of fire region from forest fire images using color rules and texture analysis," 2016 International Conference on Emerging Technological Trends (ICETT), Kollam, 2016, pp. 1-7.
- [4] Dattathreya, H. Kim, J. Park, H. Park and J. Paik, "Fire flame detection based on color model and motion estimation," 2016 IEEE International Conference on Consumer Electronics-Asia (ICCE-Asia), Seoul, 2016, pp. 1-2.
- [5] W. Dongmei, Y. Juanli, L. Baiping and L. Xiaopei, "Flame detection algorithms based on temporal-spatial visual saliency," 2015 IEEE International Conference on Signal Processing, Communications and Computing (ICSPCC), Ningbo, 2015, pp. 1-5.
- [6] S.G. Kong,D.L. Jin,S.Z. Li,H. Kim,"Fast fire flame detection in surveillance video using logistic regression and temporal smoothing,"in Fire Safety Journal,Volume 79,pp.37-43,2016.
- [7] X.Y. Zhu, Y.Y. Yan, Y.A. Liu,S.B. Gao, "Flame detection based on GBDT feature for building," 2017 International Smart Cities Conference (ISC2), Wuxi, 2017, pp. 1-5.
- [8] R. Chi, Z. M. Lu and Q. G. Ji, "Real-time multi-feature based fire flame detection in video," in IET Image Processing, vol. 11, no. 1, pp. 31-37, 1 2017.
- [9] X.Y. Wu,Y.Y. Yan,J. Du,S.B. Gao,Y.A. Liu,"Fire detection based on fusion of multiple features," in CAAI Transactions on Intelligent Systems,vol.10,no.2,pp.240-247,2015.
- [10] C. E. Prema,S.S. Vinsley,S. Suresh, "Efficient Flame Detection Based on Static and Dynamic Texture Analysis in Forest Fire Detection,"in Fire Technology, vol. 54,no.1,pp.1-34,2018.
- [11] N. Dalal and B. Triggs, "Histograms of oriented gradients for human detection," 2005 IEEE Computer Society Conference on Computer Vision and Pattern Recognition (CVPR'05), San Diego, CA, USA, 2005, pp. 886-893 vol. 1.
- [12] X.G. J, et al. "Detecting fire region based on random decision forest and HOFHOG features." in Computer Engineering & Design,no.2,pp.494-499,2017.